

# RETRIEVAL OF SURFACE DIRECTIONAL REFLECTANCE AND HEMISPHERICAL ALBEDO USING MULTI-ANGLE MEASUREMENTS

John V. Martonchik, Eric D. Danielson, David J. Diner and Carol J. Bruegge

Jet Propulsion Laboratory, California Institute of Technology  
Pasadena, CA, USA 91109

Abstract - Atmospheric correction schemes, using various levels of approximation, are described to retrieve surface bidirectional reflectance factors (BRFs) and directional hemispherical reflectances (albedos) from multi-angle radiance measurements. Observational scenarios include measurements from space-based and airborne platforms and from the ground. The retrieval schemes are tested on simulated data incorporating realistic BRFs and atmospheric models containing aerosols. It is assumed that the optical properties of the atmosphere are known well enough to model the radiative effects in the retrieval process. Sensitivity of the atmospherically-corrected BRFs and associated hemispherical reflectances to various aerosol properties and the sun-view geometry is illustrated. Keywords - atmospheric correction, surface reflectance.

## INTRODUCTION

The directional reflectance properties of natural surfaces such as soils and vegetation canopies are an essential input to the surface model inversion process [1] and the study of biospheric and atmospheric climate processes [2, 3, 4]. However, an accurate determination of surface directional reflectance requires that the radiance measurements be corrected for atmospheric effects even when the measurements are made at the surface [5]. For surface observations this correction process generally must be more sophisticated than ratioing the radiance measurements to those from a Lambertian target reflector since the directional properties of the downward diffuse radiance field are not fully accounted for by this technique.

In this paper we investigate the accuracy of various atmospheric correction schemes, ranging from rigorous to highly approximate, which were applied to simulated multi-angle data obtained for three types of observing scenarios: 1) space-based measurements with MISR (Multi-angle Imaging Spectro-Radiometer) on the EOS-AM platform to be launched in 1998, 2) airborne measurements with ASAS (Advanced Solid-State Array Spectrometer), and 3) ground level measurements with PARABOLA (Portable Apparatus for Rapid Acquisition of Bidirectional Observations of the Land and Atmosphere). It is assumed that the optical properties of the atmosphere are known, either from field measurements or inferred from the multi-angle data itself [6], so that the atmospheric radiative effects can be directly incorporated into the surface reflectance retrieval scheme. The simulated data were computed using

realistic surface bidirectional reflectance distribution functions (BRDFs) and atmospheric models containing various amounts of aerosols.

## MULTI-ANGLE RADIANCE DATA SETS

Reflectance measurements of 11 distinct types of natural surfaces in AVHRR wavelength bands 1 and 2 at 0.58-0.67  $\mu\text{m}$  and 0.73- 1.1  $\mu\text{m}$ , respectively [7-9] provided 22 distinct BRFs to be analyzed in this study. The characteristics of the BRFs are listed in Table 1.

Table 1. BRDF Characteristics

Case	Cover Type	Location	Ht (cm)	Cover (%)
1	Plowed field	Tunisia, Africa		
2	Grassland	Tunisia, Africa	< 3	<5
3	Steppe Grass	Tunisia, Africa	38	18
4	Hard Wheat	Tunisia, Africa	46	11
5	Irrigated Wheat	Tunisia, Africa	76	70
6	Hardwood forest	Beltsville, Maryland	1100	75
7	Pine forest	Beltsville, Maryland	2200	79
8	Lawn grass	Beltsville, Maryland	14	97
9	Corn	Beltsville, Maryland	33	2s
10	Soybeans	Beltsville, Maryland	77	90
11	Orchard grass	Beltsville, Maryland	22	50

The measurements were made over the entire azimuth angle range, starting from the principal plane and proceeding in 45° increments, and over the zenith angle range from 0° to 75° in 15° increments for a total of 41 measurements per solar zenith angle. The solar zenith angle coverage varied depending on the surface type but measurements were usually made at 3 or 4 different solar zenith angles within a range from 23° to 82°. A 2-dimensional cubic spline interpolation scheme then was applied to these data sets to compute the BRF at arbitrary incidence and reflection angles for use in the radiative transfer procedure. From the nature of the measurements these BRFs still contain the effects of the atmosphere. For the purposes of this study, however, it was assumed that the experimental reflection factors are the true surface BRFs.

Because surface reflectance depends on solar zenith angle, three different sun positions were investigated with zenith angles set at 25.6°, 45.9°, and 64.0°. The directional hemispherical reflectances for the 11 surface types in the two spectral bands and at the three selected sun positions were computed by

integrating the BRFs over view angle and arc displayed in the bar graph shown in Fig. 1. The smallest reflectance, 0.032, is for soybeans (case 10 in band 1 at a solar zenith angle of 45.9°) and the largest, 0.621, is for irrigated wheat (case 5 in band 2 at a solar zenith angle of 64.00).

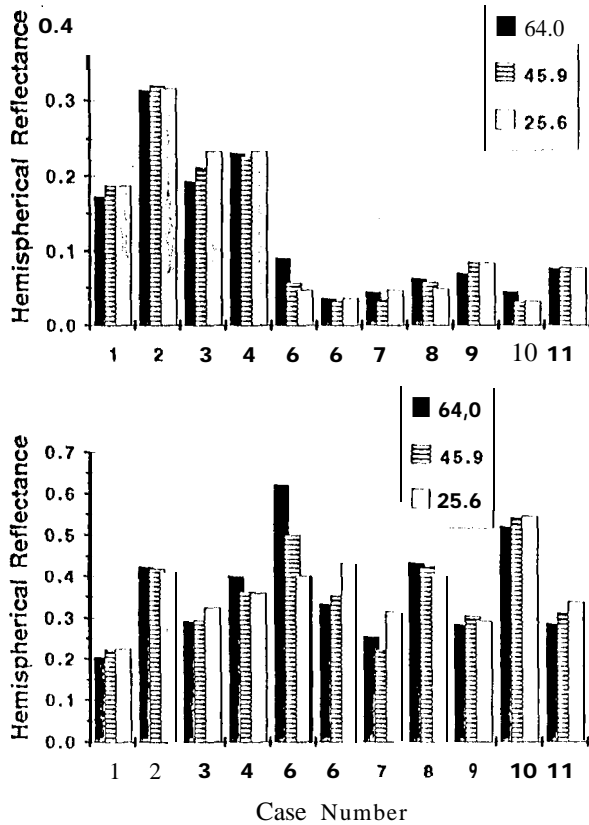


Fig. 1. Directional hemispherical reflectances of the 11 surface types in band 1 (top) and band 2 (bottom) for three solar zenith angles.

The BRFs also have a wide variety of shapes, ranging from, strong backward and forward scattering to little angular variability. For example, soil (case 1) exhibits strong backward scattering in band 1 which is highly dependent on solar zenith angle, while a pine forest (case 7) exhibits moderate forward and backward scattering in band 1 over a wide range of solar zenith angles. These two surface types represent the reflection variability extremes for the cases in Table 1 and are used as examples in the subsequent retrieval analysis.

The atmospheric model used in the radiance simulations includes the effects of both Rayleigh and aerosol scattering. The Rayleigh optical depth was set to 0.049 for band 1 and 0.010 for band 2 with a standard atmospheric scale height. The optical properties of the aerosols were assumed to be identical in bands 1 and 2. The aerosol scattering was computed using Mie theory, with a phase function described by an asymmetry parameter of 0.517 and a single-scattering albedo of 1.0. The particle density scale height was set at 2 km, not untypical of tropospheric aerosols. A number of different aerosol optical depths were considered, ranging from a low of 0.1 to a high of 0.5.

Using the 22 surface BRFs and the aerosol-laden atmospheric models described above, simulated ground-level

radiance data sets were computed for the viewing geometries of the three specified observational scenarios. The ground level radiances were spaced 45° in azimuth angle starting from the principal plane and spaced 15° in zenith angle from 00 to 75°. PARABOLANormally samples on a much finer grid but the spacing is inherently non-uniform and the data are subsequently resampled [10]. The viewing angle samplings described above is a typical resampled data set. The ASAS viewing geometry was set up with zenith angles spaced 15° from 0° to 60° and at two azimuth angles spaced by 180°. This azimuth angle separation simulates viewing in both the forward and aftward directions along the aircraft line of flight. The MISR viewing geometry is similar to the ASAS viewing geometry but with zenith angles set at 0°, 26.10, 45.6°, 60°, and 70.5° in both the forward and aftward directions. As a simplification, the simulated data sets do not include the effects of a finite view solid angle.

## RETRIEVAL APPROACH AND RESULTS

**Ground Level Observations.** The radiance reflected from a surface is a combination of direct sunlight and diffuse radiation caused by scattering of sunlight within the atmosphere. Since the atmospheric properties are assumed to be known, the reflectance measures can be inverted to obtain the surface BRF. The rigorous approach to determining the BRF of the surface is to iterate on successive BRF solutions with the diffuse radiance component being computed using the previous iteration's solution. The initial solution for the BRF is obtained by considering direct sunlight only. To achieve maximum accuracy in this retrieval process, a combined data set was used which included the reflection measurements at all three of the noted solar zenith angles. The azimuth angle of the sun,  $\phi_0$ , was placed at 0° for each of the three solar zenith angle cases. Use of the three sun angle sets together will allow a more accurate determination of the BRF since the incidence angle dependence of the BRF can be accounted for when the surface is illuminated by diffuse radiation.

For the heavily laden aerosol condition (optical depth = 0.5), the retrieved BRFs in band 1 for the 11 surface types are displayed in Fig. 2, expressed in terms of a fractional deviation  $\delta$  for each solar zenith angle. The fractional deviation  $\delta$  for a given BRF type is defined as

$$\delta(\mu_0) = \frac{1}{N} \sum_{ij} \left| \frac{r(\mu_i, \mu_0, \phi_j - \phi_0) - r_0(\mu_i, \mu_0, \phi_j - \phi_0)}{A(\mu_0)} \right| \quad (1)$$

where  $\mu, \mu_0$  are cosines of the view and sun zenith angles respectively,  $\phi - \phi_0$  is the azimuth angle measured from the principal plane,  $r$  and  $r_0$  are the retrieved and correct BRFs respectively,  $A$  is the directional hemispherical reflectance, and  $N$  is the number of unique measurements (26 for the described data sets). Although the irrigated wheat BRF (case 5) at 64.0° solar zenith angle shows a fractional deviation as high as 0.07, the average fractional deviation for the 22 BRF cases (band 2 is not shown) is under 0.03. The corresponding band 1 directional hemispherical reflectances computed from the retrieved

bidirectional reflectance factors also were shown in Fig. 2 as a percent difference from the correct values of Fig. 1. Again, the largest errors in the hemispherical reflectances reach about 7% but the average errors for all 22 BRF cases is just over 2%.

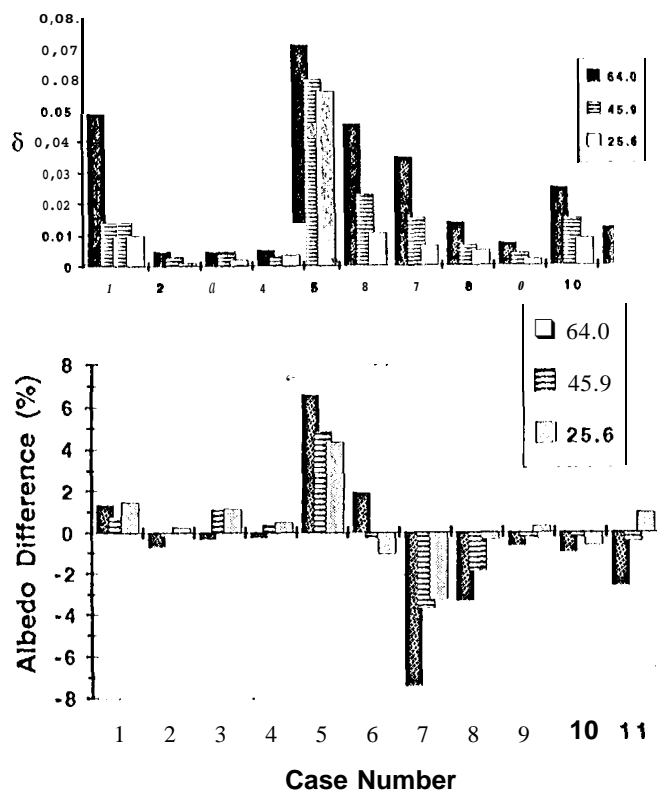


Fig. 2. (top) Fractional deviation of retrieved BRFs from true BRFs. (bottom) Hemispherical reflectance difference between computed from retrieved BRFs and true reflectances. Results are displayed for three solar zenith angles using the rigorous algorithm.

Retrievals were also done on the data sets where the aerosol loading was not so great and the results show the same trends as the heavy loading situation but with a steady improvement in accuracy with decreasing aerosol optical depth. For the data sets with an optical depth of 0.1 there is about a factor of two improvement in retrieval accuracy over those data sets with an opacity of 0.5, for both the individual BRFs and the directional hemispherical reflectances.

The technique of ratioing the measured radiances to those from an ideal Lambertian target illuminated by the same sky radiation is often used to correct the surface BRF for atmospheric effects. Fig. 3 shows the retrieval results using this approximate algorithm on those data sets produced with an aerosol opacity of 0.5. A significant reduction in accuracy, when compared to the results from the rigorous algorithm, is evident when this approximate algorithm is used. It is of interest to note that when the rigorous retrieval algorithm is used individually on the single solar zenith angle data sets, so that the approximation of no incidence zenith angle dependence of the BRF is necessary, the results are only about 30% better than those using the ratioing technique. Thus, the incidence angle dependence of the BRF must be accounted for (by means of reflection measurements at a range of solar zenith angles) when high accuracy in the

retrieval results is desired.

For those data sets produced with progressively smaller aerosol opacities, the retrieval results followed the same trends as those illustrated for the data sets with an opacity of 0.5 but with systematically increasing accuracy. The BRF retrieval results for the data sets with an aerosol opacity of 0.1, for example, were three to four times more accurate than the results in Fig. 3.

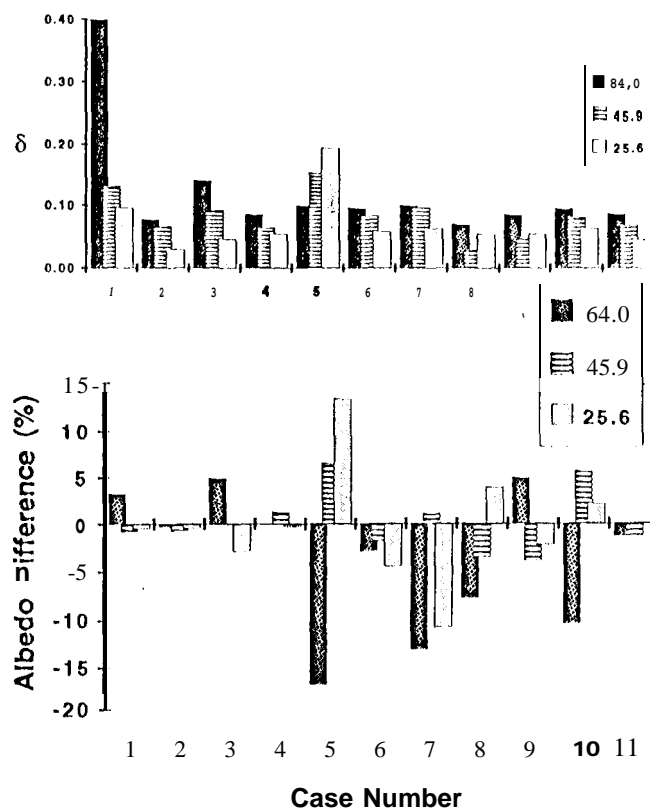


Fig. 3. Same as Fig. 2 except results were obtained using the ratioing (approximate) algorithm.

**Airborne and Space-based Observations.** Unlike ground level observations, where it is relatively easy to make reflection measurements which sample the entire hemisphere of viewing angles, airborne and space-based observations generally are restricted to a single cut in azimuth angle. This means that a number of zenith view angles can be achieved when looking in the forward motion direction and again in the backward motion direction and where there is a 180° difference in azimuth angle between the forward and aftward views. This limited angular coverage makes any surface retrieval scheme more error prone since the downward diffuse radiance component to the reflected radiance is more difficult to accurately quantify. In fact a BRF model must be used in the computations which in some measure accounts for the azimuthal variation. For this study we used a simple cosine representation,

$$r(\mu, \phi - \phi_0) = r_0(\mu) + r_1(\mu) \cos(\phi - \phi_0) \quad (2)$$

where no incidence zenith angle dependence is assumed since measurements at only a single solar zenith angle is normally obtained. There is no substantial difference in the retrieval algorithms for ASAS data and MISR data. The radiative terms in the algorithm are computed differently, however, due to the

fact that ASAS flies at an altitude of about 5 km and thus can have a non-negligible atmospheric layer above that altitude.

In Fig. 4 retrieval results are shown for MISR observations with a 45° view azimuth angle orientation to the principal plane. Again, the aerosol opacity is 0.5, and BRFs and reflectances for band 2 only are displayed for the three solar zenith angles.

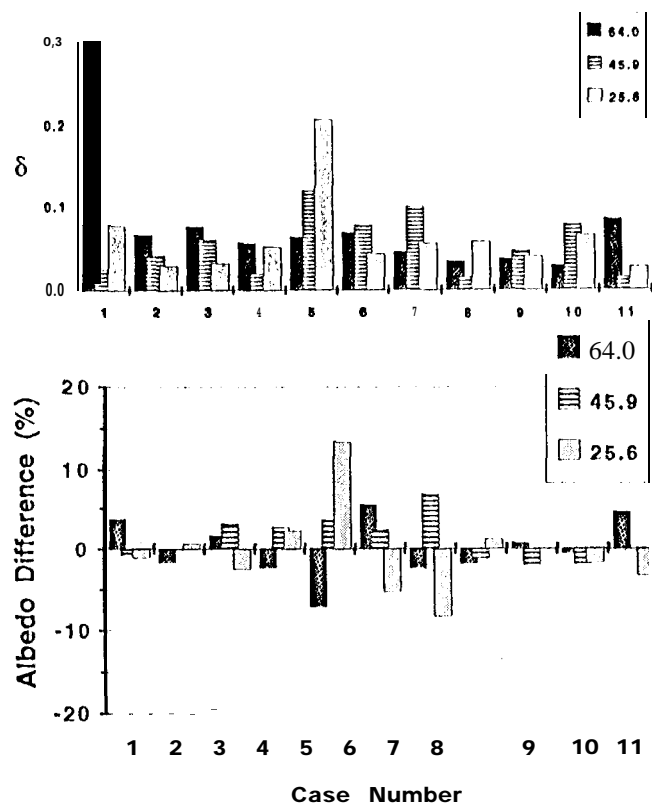


Fig. 4. Same as Fig. 2 except results were obtained using MISR data with a 45° view azimuth angle orientation to the principal plane.

An analysis of the ASAS data for the same atmospheric conditions and with the same view azimuth angles as the MISR data produces similar retrieval results. Also, like the ground level retrievals, when the optical depth of the atmosphere decreases the retrieved BRFs and hemispherical reflectances show a corresponding improvement in accuracy.

#### 1)1 SCUSSION ANI CONCLUSION

The correction of surface directional reflectance measurements for atmospheric effects can be accomplished in a direct way provided the necessary atmospheric parameters are known so that the associated radiative properties can be determined. For ground level measurements it is possible to obtain excellent coverage of viewing angle over the hemisphere. However, for BRFs with a strong solar zenith angle dependence it is also necessary to obtain reflection measurements for a wide range of solar zenith angles when high accuracy is required of the retrieval process. This is especially true when atmospheric optical depths are about 0.3 and greater because of the large diffuse field contribution to the reflected radiation. The retrieval of the BRF tends to be more susceptible to error than the hemispherical reflectance because the angle integrating process for computing reflectance tends to average out positive and

negative errors in the BRF.

Surface retrievals using directional reflectance measurements made from airborne and space-based platforms are inherently less accurate than retrievals using ground level measurements. This is due to both the limited azimuth angle and the solar zenith angle coverage. However, even when the measurements are made at only two azimuth angles and a single zenith angle, the retrieval can produce quite acceptable accuracies. It is anticipated that if a parametrized physical model is incorporated into the retrieval process the accuracy can be improved significantly.

**Acknowledgement.** This research was carried out by the Jet Propulsion Laboratory, California Institute of Technology, under contract with the National Aeronautics and Space Administration.

#### REFERENCES

- [1] B. Pinty and M.M. Verstraete, "On the Design and Validation of Surface Bidirectional Reflectance and Albedo Models," *Remote Sens. Environ.*, VOI.41, pp. 155-167, 1992.
- [2] J. G. Charney, W.G. Quirk, S.M. Chow, and J. Kornfield, "A Comparative Study of the Effects of Albedo Change of Drought in Semi-arid Regions," *J. Atmos. Sci.*, vol.34, pp. 1366-1385, 1977.
- [3] Y. Mintz, "The Sensitivity of Numerically Simulated Climates to Land-Surface Conditions," in *The Global Climate*, ed. J. Houghton, Cambridge, London, New York: Cambridge University Press, 1984.
- [4] R.E. Dickinson, "Land Surface Processes and Climate-Surface Albedos and Energy Balance," *Adv. Geophys.*, vol.25, pp.305-353, 1983.
- [5] D.W. Deering and T.F. Eck, "Atmospheric Optical Depth Effects On Angular Anisotropy of Plant Canopy Reflectance," *Int. J. Remote Sensing*, VOI.8, pp.893-916, 1987.
- [6] J.V. Martonchik and D.J. Diner, "Retrieval of Aerosol Optical Properties from Multi-Angle Satellite Imagery," *IEEE Trans. Geosci. Remote Sensing*, vol.30, pp.223-230, 1992.
- [7] D.S. Kimes, "Dynamics of Directional Reflectance Factor Distributions for Vegetation Canopies," *Appl. Opt.*, vol.22, pp.1364-1372, 1983.
- [8] D.S. Kimes, W.W. Newcomb, R.F. Nelson, and J. H. Schutt, "Directional Reflectance Distributions of a Hardwood and Pine Forest Canopy," *IEEE Trans. Geosci. Remote Sens.*, vol. GE-24, pp.281-293, 1985.
- [9] D.S. Kimes, W.W. Newcomb, C.J. Tucker, I.S. Zonneveld, W. Van Wijngaarden, J. de Leeuw, and G.F. Epema, "Directional Reflectance Factor Distributions for Cover Types of Northern Africa in NOAA 7/8 AVF 1 RR Bands 1 and 2," *Remote Sens. Environ.*, vol. 18, pp. 1-19, 1985.
- [10] S.P. Ahmad, E.M. Middleton and D.W. Deering, "Computation of Diffuse Sky Irradiance from Multidirectional Radiance Measurements," *Remote Sens. Environ.*, VOI.21, pp. 185-200, 1987.